European Spine Journal (2019) 28:2198–2207
https://doi.org/10.1007/s00586-019-06012-2

ORIGINAL ARTICLE

Supplementary delta-rod configurations provide superior stiffness and reduced rod stress compared to traditional multiple-rod configurations after pedicle subtraction osteotomy: a finite element study

Pedro Berjano[1] · Ming Xu[2] · Marco Damilano[1] · Thomas Scholl[2] · Claudio Lamartina[1] · Michael Jekir[2] · Fabio Galbusera[1]

Received: 9 September 2018 / Revised: 15 March 2019 / Accepted: 13 May 2019 / Published online: 25 May 2019

Abstract

Purpose The biomechanical performance of conventional multi-rod configurations (satellite rods and accessory rods) in pedicle subtraction osteotomies has been previously studied in vitro and using finite element models (FEM). Delta and delta-cross rods are innovative multi-rod configurations where the rod bends were placed only in its proximal and distal extremities in order to obtain a dorsal translation of the central part of the rod respect to the most angulated area of the main rods. However, the biomechanical properties of the delta and delta-cross rods have not been investigated. This study used FEM to analyze the effect of delta-rod configurations on the stiffness and primary rod stress reduction in multiple-rod constructs after pedicle subtraction osteotomy.

Methods The global range of motion in the spine and the magnitude and distribution of the von Mises stress in the rods were studied using a spine finite element model described previously. A follower load of 400 N along with moments of 7.5 N in flexion/extension, lateral bending, and axial rotation were tested on the spine model. Initial breakage was created on the rod based on the maximum stress location. The post-breakage models were tested under flexion.

Results Delta and delta-cross rods reduced more range of motion (up to 45% more reduction) and reduced more primary rod stress than other previously tested rod configurations (up to 48% more reduction). After initial rod fracture occurred, delta and delta-cross rods also had less range of motion (up to 23.6% less) and less rod von Mises stress (up to 81.2% less) than other rod configurations did.

Conclusions Delta and delta-cross rods have better biomechanical performance than satellite rods and accessory rods in pedicle subtraction osteotomies in terms of construct stiffness and rod stress reduction. After the initial rod breakage occurred, the delta and delta-cross rods could minimize the loss of fixation, which have less rod stress and greater residual stiffness than other rod configurations do. Based on this FEA study, delta-rod configurations show more favorable biomechanical behavior than previously described multi-rod configurations.

Electronic supplementary material The online version of this article (https://doi.org/10.1007/s00586-019-06012-2) contains supplementary material, which is available to authorized users.

✉ Ming Xu
mingxuttu@gmail.com

[1] IRCCS Istituto Ortopedico Galeazzi, Milan, Italy

[2] NuVasive, Inc., San Diego, CA, USA

Graphical abstract

These slides can be retrieved under Electronic Supplementary Material.

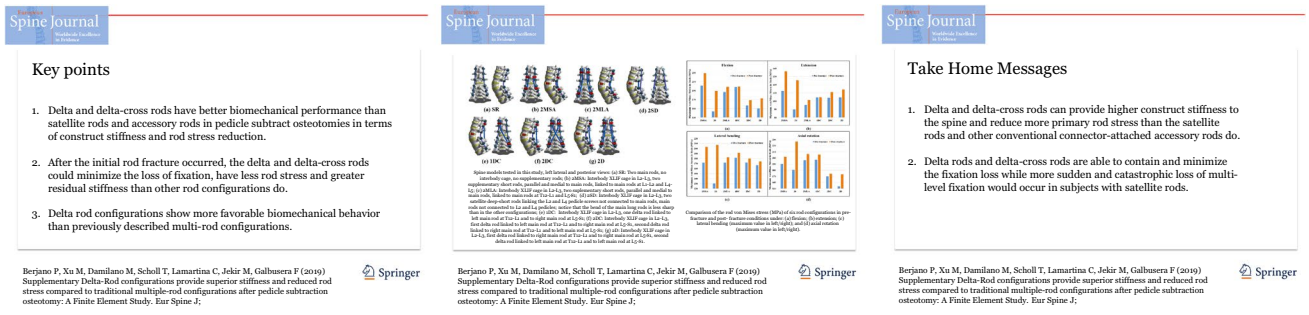

Keywords Pedicle subtraction osteotomy · Multi-rod fixation · Range of motion · Rod von Mises stress · Finite element analysis · Post-fracture

Introduction

Pedicle subtraction osteotomy (PSO) has been widely used to achieve significant alignment corrections in adult deformity, which may achieve a lordosis angle up to 30°–35° at one single level [1–4]. Rod fracture is one concerning complication related to PSO, which can cause loss of posterior fixation and correction, pain, and neurological impairment [5, 6]. Revision surgery is often required after the rod fracture [7–9]. Different approaches have been introduced to improve the rod survival rate in PSO, such as bone-to-bone osteotomies [10], multiple-rod configurations [11, 12], adding interbody (IB) cage adjacent to PSO level [13], and utilization of cobalt chrome rods as alternative to titanium rods [14]. In PSO with multi-rod configurations, accessory rods and satellite rods proved to reduce the rod stress and increase the stability of the fixation [15–17].

Most of the multiple-rod configurations proposed in the past have in common the uniplanar configuration with position of all the rods at a close sagittal distance to a common frontal plane. Past experience derived from external fixation for limb fractures or reconstruction with the Hoffmann external fixation frame has shown how multi-planar constructs have substantial mechanical advantages in terms of stiffness and resistance to failure [18, 19].

The first author (PB) introduced the concept of delta rod (DR) for revision cases in rod failure after three-column osteotomy (3CO). Delta rod was defined as a configuration where one or two accessory rods were connected to the main rods around a 3CO, avoiding bending the third and fourth rods with exact matching of the sagittal shape of the main rods. Instead of this, the rod bends were placed only in its proximal and distal extremities in order to obtain a dorsal translation of the central part of the rod respect to the most angulated area of the main rods (Fig. 1).

Finite element models (FEMs) reproduce well the behavior of the intact and instrumented spine and allow studying and comparing the effects of different instrumentation constructs [20]. The objective of this study is to compare, by means of FEM, the mechanical properties of various DR configurations to other conventional rod configurations after PSO regarding construct stiffness and rod stress. The second aim of the study is to compare the residual mechanical properties of the constructs after primary rod breakage.

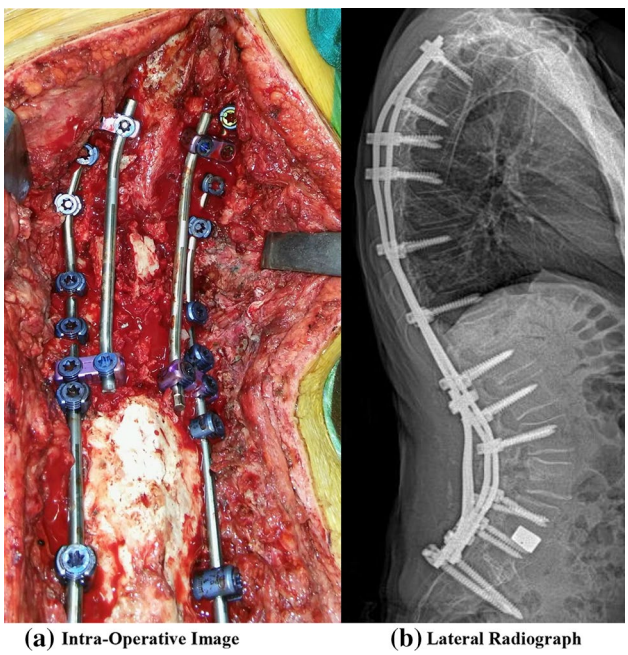

Fig. 1 Delta-rod configurations: **a** posterior intra-operative image of delta configuration; **b** lateral radiograph of delta configuration

Materials and methods

In a previous study, a nonlinear three-dimensional FEM spine model of T12-sacrum was developed and validated. Details of the model and validation have been described elsewhere [15]. The range of motion predicted by the spine FEM was validated against a cadaveric experimental test.

The models of pedicle screw and rod were created in PTC Creo Parametric 2.0 (PTC, Needham, MA). The screws have an outer diameter of 6.5 mm and were made from titanium alloy (Ti6Al4V) with a Young's modulus of 113.8 GPa and a Poisson's ratio of 0.3. The rods have a diameter of 5.5 mm and were made from cobalt–chromium with a Young's modulus of 210 GPa and a Poisson's ratio of 0.29. The pedicle screws and the rod connectors were meshed by tetrahedral elements, and the rod was meshed by hexahedral elements in Hyperworks (Altair Engineering Inc., Troy, MI, USA). The connection between the rod and connector, connection between the screw and vertebra, and connection between the screw and rod were simulated as bonded contacts where no relative movement is permitted between the contacting surfaces. The contact between the interbody cage and endplates was simulated as bonded contact, which didn't allow separation and sliding at the contact surface. The simulations were performed in ANSYS R18.0 (ANSYS Inc., Canonsburg, PA, USA).

The FEM of the spine was modified with a 25° PSO at L3 as previously described [15]: The osteotomies were created by removing all the posterior elements of L3 using a 25° wedge and then closing the osteotomy. The spine FEM was instrumented with bilateral pedicle screws at each level from T12 to L2 and L4 to S1, interbody XLIF cage at L2–L3, and supplementary rods connected to the main rods in two points. The primary rods were contoured to follow the spinal curvature.

The following PSO rod configurations were simulated in the FEM (Fig. 2):

(a) Single rod with PSO (without L2–L3 cage) (SR);
(b) Bilateral medial short auxiliary rods (2MSA);
(c) Bilateral medial long auxiliary rods (2MLA);
(d) Bilateral short-deep satellite rods (2SD);
(e) Single cross delta rod (1DC);
(f) Double cross delta rod (2DC);
(g) Bilateral medial delta rods (2D).

Each spine model was preloaded with a follower load of 400 N using connector elements along the spinal curvature in combination of pure moments of 7.5 Nm in flexion,

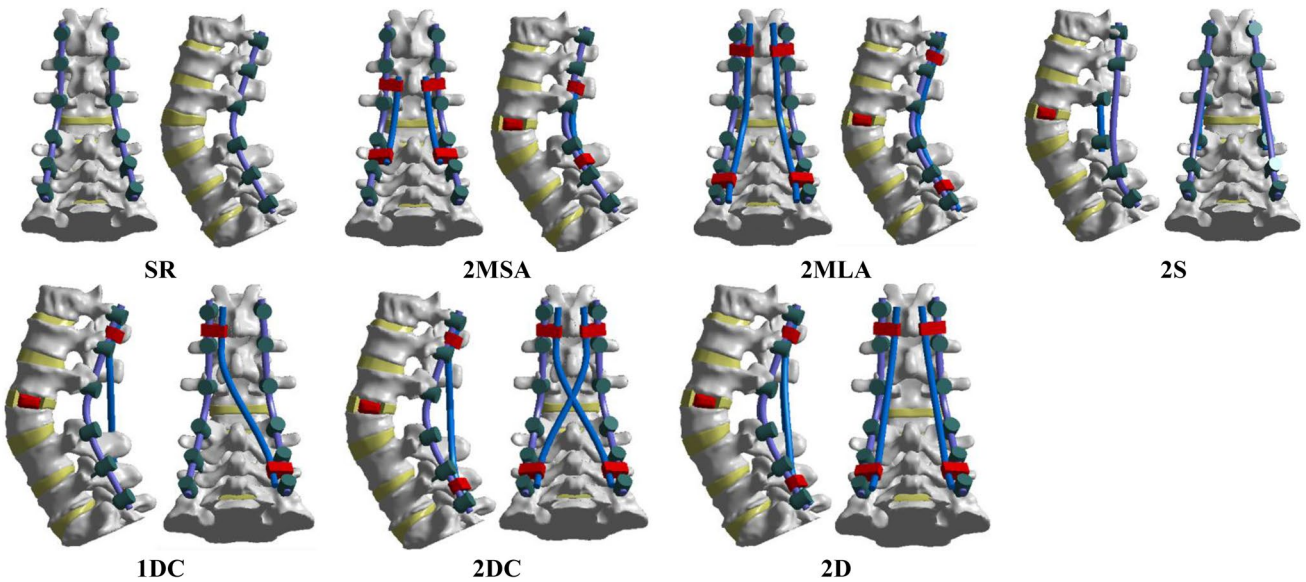

Fig. 2 Spine models tested in this study, left lateral and posterior views: **a** SR: Two main rods, no interbody cage, no supplementary rods; **b** 2MSA: interbody XLIF cage in L2–L3, two supplementary short rods, parallel and medial to main rods, linked to main rods at L1–L2 and L4–L5; **c** 2MLA: interbody XLIF cage in L2–L3, two supplementary short rods, parallel and medial to main rods, linked to main rods at T12–L1 and L5–S1; **d** 2S: interbody XLIF cage in L2–L3, two satellite deep-short rods linking the L2 and L4 pedicle screws not connected to main rods, main rods not connected to L2 and L4 pedicles; notice that the bend of the main long rods is less sharp than in the other configurations; **e** 1DC: interbody XLIF cage in L2–L3, one delta rod linked to left main rod at T12–L1 and to right main rod at L5–S1; **f** 2DC: interbody XLIF cage in L2–L3, first delta rod linked to left main rod at T12–L1 and to right main rod at L5–S1, second delta rod linked to right main rod at T12–L1 and to left main rod at L5–S1, no contact between the two cross rods; **g** 2D: interbody XLIF cage in L2–L3, first delta rod linked to right main rod at T12–L1 and to right main rod at L5–S1, second delta rod linked to left main rod at T12–L1 and to left main rod at L5–S1

extension, lateral bending, and axial rotation applied at the superior endplate of T12 [21]. The sacrum was constrained in all degrees of freedom. In the 2DC configuration, no contact between the two cross rods was defined.

The maximum von Mises stresses in the rods were measured for each rod configuration and loading condition. The locations where the maximum stress occurred on the rods were also compared for all the configurations. The global range of motion (ROM) of L1–S1 spine levels was measured for flexion, extension, left/right lateral bending, and left/right axial rotation.

First, the ROM of the spine, the magnitude of maximum values, and distribution of von Mises stress in the rods were recorded and compared. Secondly, to investigate the rod stress after fracture in the rods occurs, the elements at the maximum stress locations predicted in previous simulations were removed from the model to simulate rod fracture. The first layer of element surrounding the highest stress was removed. Post-fracture models were generated for six configurations tested in this study: 2MSA, 2MLA, 1DC, 2DC, 2D, and 2S. A preload of 400 N and a flexion moment of 7.5 Nm were applied on the post-fracture models. The magnitude and distribution of von Mises stress in the rods and the global ROM of the spine in the post-fracture models were calculated and compared with those in the pre-fracture conditions.

Results

Range of motion

The change in ROM was calculated for each of the rod configurations compared to that in SR model (Table 1). In the previous study [15], the configuration with highest stiffness (champion configuration) after PSO with interbody cage was the addition of two short satellite rods (2S: up to − 45%), followed by the addition of two long accessory rods linked to the main rod (2MLA: up to − 36%). In the present test, all the delta configurations showed stiffness superior to the champion configuration of the previous study (SD). Furthermore, the stiffest configuration was the delta double cross (2DC: up to − 52%). Longer accessory rods performed better (2MLA: up to − 36%) than the short accessory rods did (2MSA: up to − 19%). In lateral bending and axial rotation, delta-cross rods and delta (D) rods had the most emerging advantage over conventional accessory rods (up to − 41% more ROM reduction).

von Mises stress in the rod

The stress variation in the rods was calculated relative to the PSO condition (Table 2). In the previous study [15], the configuration with lowest rod von Mises stress (champion configuration) after PSO with interbody cage was the addition of two deep-short satellite rods (2S: up to − 50%),

Table 1 Comparison of range of motion change in primary rods in different rod configurations relative to that in PSO

Configuration	Flexion	Extension	Right lateral bending	Left lateral bending	Right axial rotation	Left axial rotation
SR	3.2°	0.5°	2.0°	2.0°	2.8°	2.8°
2S	− 20%	− 45%	− 16%	− 16%	− 15%	− 15%
2MSA	− 14%	− 1%	− 11%	− 11%	− 19%	− 19%
2MLA	− 25%	− 14%	− 22%	− 22%	− 36%	− 36%
1DC	− 25%	− 51%	− 31%	− 43%	− 49%	− 23%
2DC	− 39%	− 46%	− 52%	− 52%	− 49%	− 49%
2D	− 41%	− 47%	− 26%	− 26%	− 45%	− 45%

Table 2 Comparison of maximum von Mises stress change in primary rods in different rod configurations relative to that in PSO

Configurations	Flexion	Extension	Right lateral bending	Left lateral bending	Right axial rotation	Left axial rotation
SR	286 MPa	92 MPa	228 MPa	228 MPa	247 MPa	247 MPa
2S	− 50%	− 2%	− 43%	− 43%	− 27%	− 27%
2MSA	− 29%	34%	− 16%	− 16%	− 20%	− 20%
2MLA	− 35%	4%	− 25%	− 25%	− 20%	− 20%
1DC	− 31%	− 14%	− 20%	− 27%	− 30%	− 20%
2DC	− 45%	− 13%	− 25%	− 25%	− 31%	− 31%
2D	− 48%	− 14%	− 27%	− 27%	− 38%	− 38%

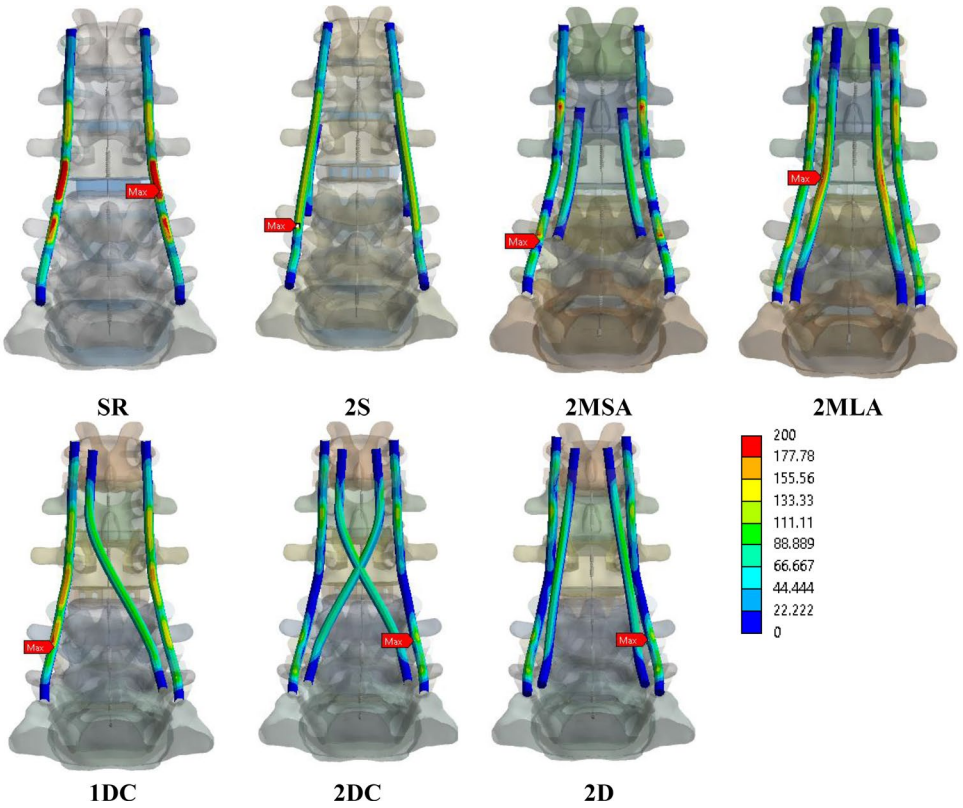

Fig. 3 Comparison of von Mises stress distribution in the rods in different configurations under flexion. The stress color bar is scaled to 0–200 MPa for all configurations. Maximum stress location marked in red

followed by the addition of two long accessory rods linked to the main rod (2MLA: up to − 35%). In the present test, compared with the champion configuration in the previous study (SC), double DC rods and D rods showed equivalent primary rod stress reduction in flexion (2S: − 50%, 2DC: − 45%, 2D: − 48%), more primary rod stress reduction in extension (2S: − 2%, 2DC: − 13%; 2D: − 14%) and axial rotation (2S: − 27%, 2DC: − 31%; 2D:− 38%) but less stress reduction in lateral bending (2S: − 43%, 2DC: − 25%; 2D: − 27%). The double DC rods and D rods produced substantially more primary rod stress reduction than all the conventional accessory rod configurations under all loading conditions. Among all the loading conditions, flexion produced the highest primary rod von Mises stress in all rod configurations, which identified flexion as worst-case loading condition.

As shown in Fig. 3, during flexion (worst-case loading condition), the maximum von Mises stress occurred at the root of connector or pedicle screw in primary rod outside the osteotomy level in all supplemented-rod configurations after PSO except for the long accessory rods. In the non-supplemented PSO configuration and the configuration with long conventional accessory rods, the maximum von Mises stress occurred at the osteotomy level [15].

Post-fracture models

As flexion is the worst-case loading mode, the post-fracture models were generated by removing elements at fracture location in the primary rods where the maximum von Mises stress occurred during flexion. The post-fracture models were tested under flexion/extension, left/right lateral bending, and left/right axial rotation.

As shown in Fig. 4, after the initial breakage, satellite rods had up to 59.2% (in lateral bending) increase in rod von Mises stress, whereas DC rod had rod von Mises stress increase of only up to 7.6% (in flexion) and 2D rods had up to 15.3% increase (in flexion). As a result, single DC rod produced up to 16.6% (in extension) lower rod von Mises stress than satellite rods did while double DC rods produced up to 23.2% (in axial rotation) and double D rods produced up to 23.6% (in axial rotation) lower primary rod von Mises stress than satellite rods did.

As shown in Fig. 5, after the initial breakage, satellite rods had up to 440.8% (in lateral bending) increase in ROM, whereas double DC rod had ROM increase of up to 13.6% (in lateral bending) and double D rods had up to 22.7% increase (in axial rotation). As results, single DC rod produced up to 76.5% (in extension) lower ROM than satellite rods did while double DC rods produced up to 79.9% (in extension) and double D rods produced up to 81.2% (in extension) lower ROM than satellite rods did.

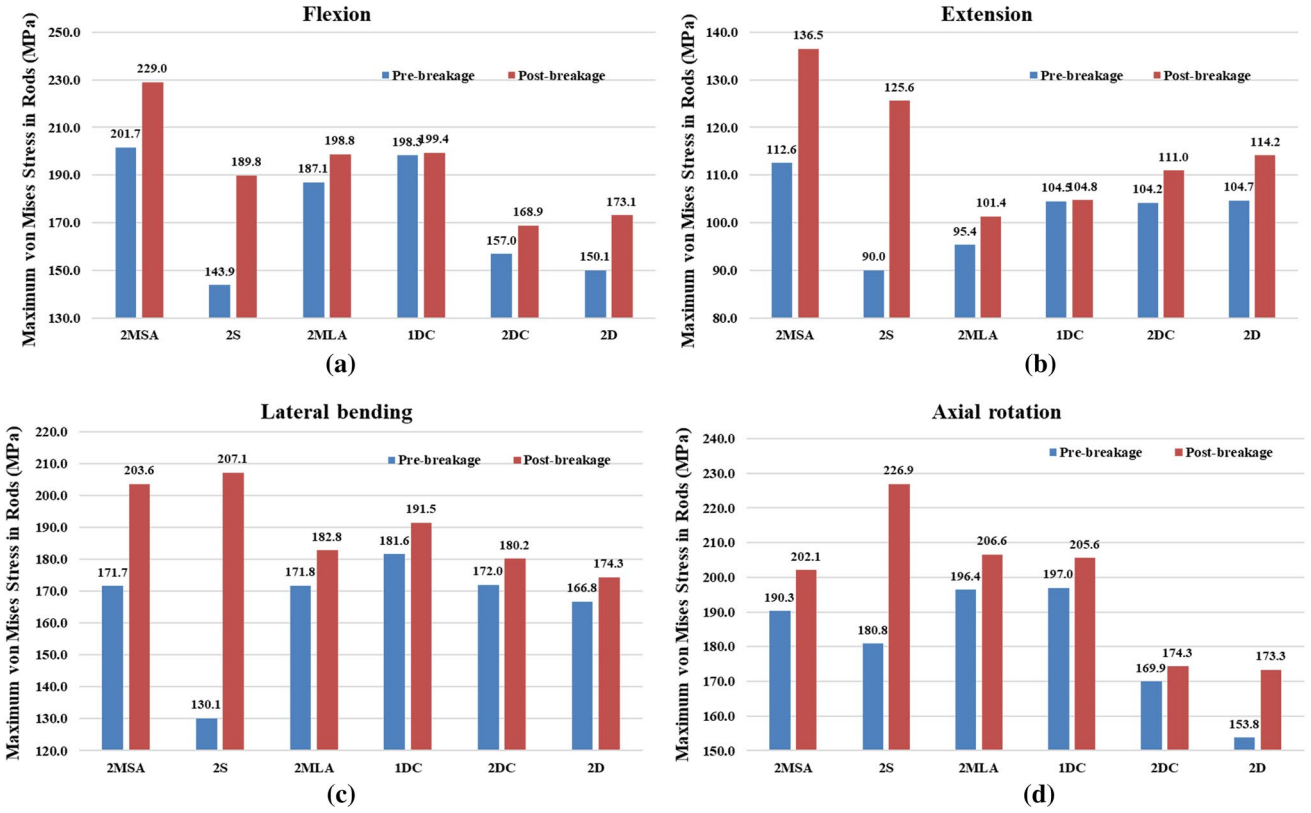

Fig. 4 Comparison of the rod von Mises stress (MPa) of six rod configurations in pre-fracture and post-fracture conditions under: **a** flexion; **b** extension; **c** lateral bending (maximum value in left/right); and **d** axial rotation (maximum value in left/right)

After rod fracture (Fig. 5), the fracture area became unstressed and not load-bearing while the stress in the contralateral side substantially increased. The new maximum stress location shifted to the non-fractured rods, while approximately maintaining the same location in the rod. In the PSO with satellite rods configuration, the unstressed area on the fractured rod was between the pedicle screws on L2 and L5. In PSO with long accessory rods, the unstressed area on the broken rod was between the connectors on T12–L1 and on L5–S1. With DC rods and D rods, the unstressed area on the fractured rod was contained to only one level.

Discussion

In the present study, we compared the PSO supplemented with D and DC rods with the PSO with conventional accessory rods and satellite rods. The global ROM of the spine model reflected the stiffness of the spine and the von Mises stress in the rod can gauge the risk of rod fracture. It is not feasible to measure the continuous stress distribution in the rod using physical tests, but strain in the rod can be measured at discrete locations in the rod using experimental studies [15–17, 22]. This study also investigated the stress distribution on the rods during different loading conditions. The spine FEM we employed in this study was previously validated, and the findings provided by these models proved to be well consistent with clinical observations [15].

Since the bending moments applied on the spine models are constant among all the configurations, comparing the relative ROM can reflect the stiffness among different rod configurations. Our previous study showed satellite rods reduced more stress in the primary rods than other rod configurations did after PSO [15]. The present study showed that PSO supplemented with 2D and 2DC rods reduced more ROM than PSO with conventional accessory rods/satellite rods did in all loading conditions. Due to the high lordosis created by PSO, higher spinal loads were placed on the posterior column of the spine. Thus, considerably more load is transferred to the posterior fixators after PSO [11]. This study hypothesized that 2D and 2DC rods have a more favorable load path than the highly angulated conventional accessory rods do because they provide more straight axial support bridging the superior and inferior parts of the construct and are in a more posterior position shielding the primary rods in PSO level. D and DC rods increased construct stiffness at the PSO level; therefore, the rod stress is reduced. This hypothesis should be further investigated in

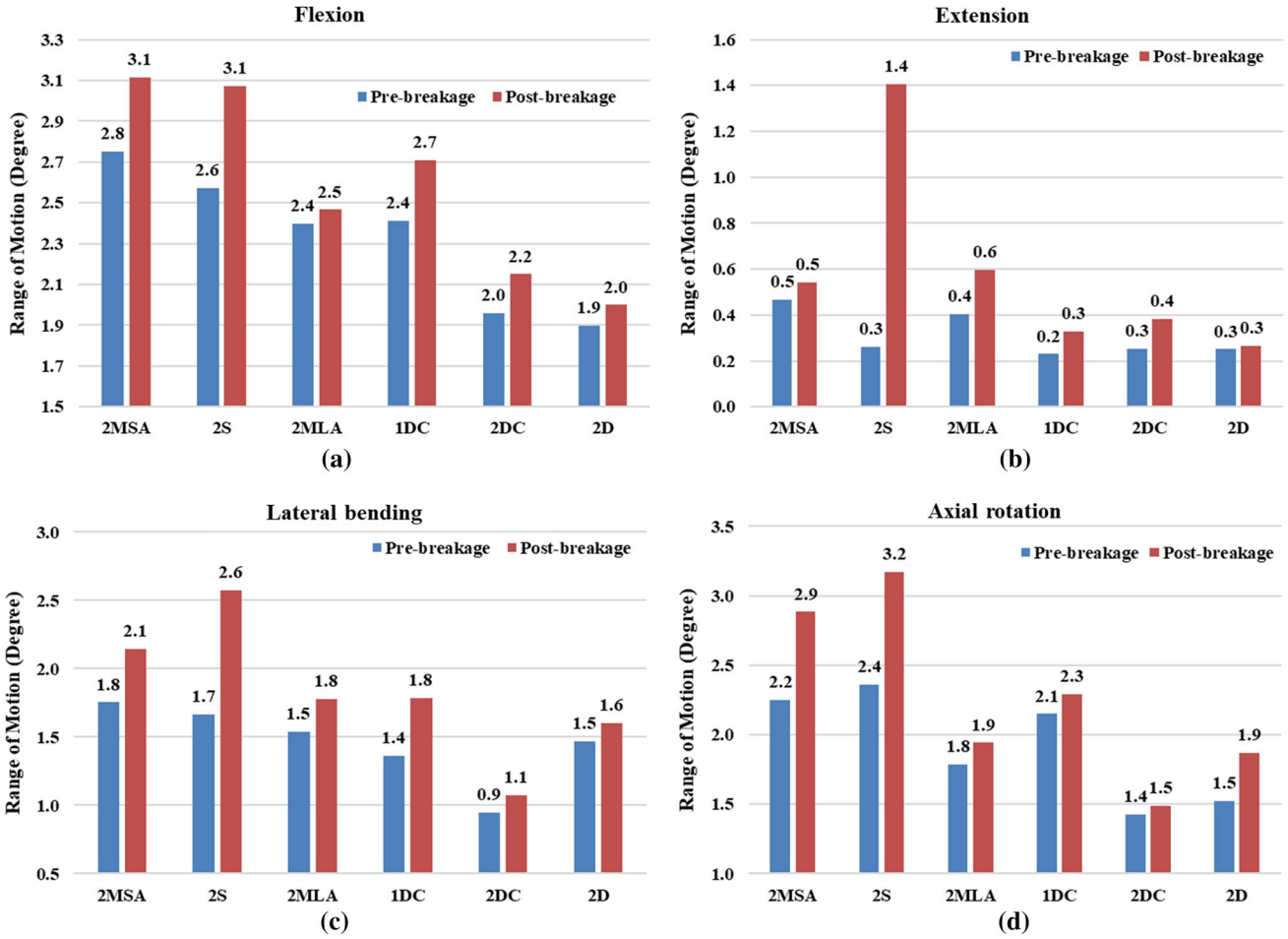

Fig. 5 Comparison of the global range of motion (degree) of six rod configurations in pre-fracture and post-fracture conditions under: **a** flexion; **b** extension; **c** lateral bending (maximum value in left/right); and **d** axial rotation (maximum value in left/right)

the clinical studies and cadaveric studies. This could explain the considerable fixation stiffness increase provided by delta and cross rods. More importantly, DC rods provide transverse connection between two primary rods without requiring additional transverse connectors. This unique "transverse bridging effect" provided by 2DC can explain the spinal stability improvement provided in axial rotation.

In terms of rod von Mises stress, our FEA results indicate that PSO with DC rods and D rods reduced considerably more rod stress than conventional accessory rod in all loading conditions (up to 18% more). The DC and D rods also reduced more primary rod stress than satellite rods did during axial rotation and extension and produced comparable primary rod stress reduction in flexion. Maximum rod stress concentrated at the root of connector/rod attaching areas in configurations with both conventional accessory rods and cross and delta rods (Fig. 6). In the configurations with satellite rods, since no rod connectors attached to the primary rods, less stress concentration effect occurred and the primary rod stress tended to be more distributed. This finding is consistent with those reported by previous studies [17, 23]. This can also explain the reason why the satellite rods reduced more rod stress than rod-connector-attached accessory rods did. Since DC and D rods also used rod connectors attaching the primary rods, stress concentration occurred at the root of connector in primary rods. Even with such stress concentration, it is interesting to observe that the DC and D rods were comparable or superior to the satellite rods in terms of the primary stress reduction. Overall, considering the superior ROM and rod stress reduction provided by the DC and D rods, DC and D rods have demonstrated biomechanical advantage over conventional accessory rods and satellite rods in PSO subjects.

Assuming the initial rod fracture occurs at the location of maximum von Mises stress in pre-breakage condition, the post-breakage rod stress and stiffness of the fixation were simulated by generating the breakage in the rod at that point. After the breakage, DC and D rods had tremendous advantage over the satellite rods in terms of both rod von Mises stress and ROM. Since the satellite rods were not attached to

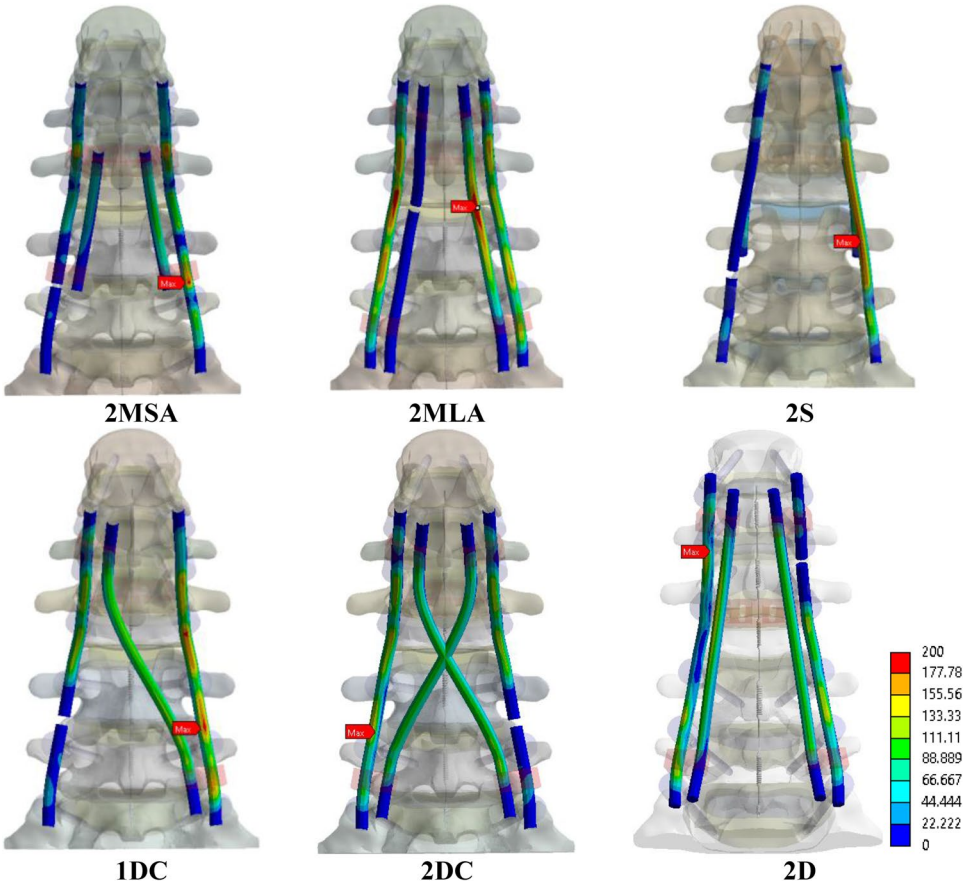

Fig. 6 Comparison of von Mises stress distribution in the rods in different configurations after fracture in rods under flexion. The stress color bar is scaled to 0–200 MPa for all configurations. Red arrows indicate maximum von Mises stress location

the primary rods, the satellite rods could not provide support to the breakage area on the primary rods, whereas D and DC rods could cover the breakage area and reduce the loss of fixation. In PSO with satellite rods, the broken rod lost three levels of fixation on one side while PSO delta-cross rods and delta rods only lost 1 level of fixation on one side. Thus, D and DC rods could minimize the loss of fixation after the initial rod fracture occurs and reduce the risk of further breakage. Conversely, in satellite rod configurations, the immediate loss of multi-level fixation might result in catastrophic further failure in the fixation.

Limitations of this study should be considered. First, the contacts between rod and rod connectors and between the rod and screws were simplified as a bonded connection, where no relative movement is allowed at the contact surface. This might magnify the stress concentration effect on the rods, which might make the absolute stress value predicted in this study slightly higher than that in physical or cadaveric study. However, since this study focused on comparing different rod configurations relative to each other, and since continuous rod stress is not feasible to measure using experimental study, the utilized contact definition served the context of use of this study. Second, cyclic loading test was not performed in this study and the alternating stress on the rods was not calculated. It would also be interesting to simulate the cyclic loads on the rod configurations in this study using test blocks similar to ASTM F1717 setup [24], which is currently ongoing. Future clinical study is also required to further investigate the long-term effect of the delta and cross rods tested in this FEA study. Third, adding anterior support like interbody cage might also reduce the load and stress in the posterior fixation [25, 26]. However, the focus of this study is on the configurations of the posterior fixation. The interbody cage condition is kept consistent among different rod configurations. Fourth, the notch effect on the rods was not addressed in this study. It is challenging to measure or simulate the notch condition on the rod in experimental or computational study since great variations in surface condition exist. However, since no stress concentration was observed in the most bended area in the delta rod in this study, the notch effect won't affect the worst-case configuration prediction in this study. To the best of our knowledge, no study has been performed to investigate notch effect on the rod. We will investigate the notch effect on the rods in the future study. Fifth, the anatomical compatibility should be considered before utilizing D and DC rod configurations in clinical practice. However, this study mainly focuses on investigating the biomechanical performance of the D and DC rods. The anatomical compatibility will be investigated in future studies.

Conclusion

This study indicates that the D and DC rods can provide higher construct stiffness to the spine and reduce more primary rod stress than the satellite rods and other conventional connector-attached accessory rods do. After rod fracture occurred in PSO subjects, D rods and DC rods are able to contain and minimize the fixation loss while more sudden and catastrophic loss of multi-level fixation would occur in subjects with satellite rods. Based on this FEA study, delta-rod configurations show more favorable biomechanical behavior than previously described multi-rod configurations.

Compliance with ethical standards

Conflict of interest Dr. Pedro Berjano has received grants from NuVasive, DePuy Synthes, K2M, Speaker honorarium from Medacta and NuVasive. Dr. Ming Xu is former employee of NuVasive and owns stock of NuVasive. Mr. Thomas Scholl and Mr. Michael Jekir are current employees of NuVasive and own stock of NuVasive. Dr. Marco Damilano has received grants from NuVasive and K2M No honorarium for speaker. Dr. Claudio Lamartina is consultant for Depuy-Sythes, K2M, Medacta, NuVasive, Sintea, Zimmer, Deputy Editor for clinical science of European Spine Journal, and past chairman of AOSpine Board of Europe and Africa.

References

1. Bridwell KH, Lewis SJ, Lenke LG (2003) Pedicle subtraction osteotomy for the treatment of fixed sagittal imbalance. J Bone Jt Surg Am 85:454–463
2. Dickson DD, Lenke LG, Bridwell KH, Koester LA (2014) Risk factors for and assessment of symptomatic pseudarthrosis after lumbar pedicel subtraction osteotomy in adult spinal deformity. Spine 39(15):1190–1195
3. Berjano P, Zanirato A, Compagnone D, Redaelli A, Damilano M (2018) Hypercomplex pedicle subtraction osteotomies: definition, early clinical and radiological results and complications. Eur Spine J 27(1):115–122
4. Berjano P, Damilano M, Langella F, Pejrona M, Lamartina C (2014) Osteotomies of the spine:"Technique of the Decade"? Eur Spine J 24(1):1–2
5. Berjano P, Bassani R, Casero G, Sinigaglia A, Cecchinato R, Lamartina C (2013) Failures and revisions in surgery for sagittal imbalance: analysis of factors influencing failure. Eur Spine J 22(6):853–858
6. Zanirato A, Damilano M, Formica M, Piazzolla A, Lovi A, Villafane JH, Bernjano P (2018) Complications in adult spine deformity surgery: a systematic review of the recent literature with reporting of aggregated incidences. Eur Spine J 27(9):2272–2284
7. Smith JS, Sansur CA, Donaldson WF, Perra JH, Mudiyam R, Choma TJ, Zeller RD, Knapp DR, Noordeen HH, Berven SH, Goytan MJ, Boachie-Adjei O, Shafferey CI (2011) Short-term morbidity and mortality associated with correction of thoracolumbar fixed sagittal plane deformity. Spine 36(12):958–964
8. Berjano P, Pejrona M, Damilano M, Cecchinato R, Aguirre MFI (2015) Corner osteotomy: a modified pedicle subtraction osteotomy for increased sagittal correction in the lumbar spine. Eur Spine J 24(1):58–65
9. Charles YP, Yu B, Steib JP (2016) Sacroiliac joint luxation after pedicle subtraction osteotomy: report of two cases and analysis of failure mechanism. Eur Spine J 25(Suppl 1):63–74
10. Smith JS, Shaffrey E, Klineberg E, Shaffrey CI, Lafage V, Schwab FJ, Protopsaltis T, Scheer JK, Mundis GM, Fu K-MG, Gupta MC, Hostin R, Deviren V, Kebaish K, Hart R, Burton DC, Line B, Bess S, Ames CP (2014) Prospective multicenter assessment of risk factors for rod fracture following surgery for adult spinal deformity. J Neurosurg Spine 21(6):994–1003
11. Palumbo MA, Shah KN, Eberson CP, Hart RA, Daniels AH (2015) Outrigger rod technique for supplemental support of posterior spinal arthrodesis. Spine J 15(6):1409–1414
12. Hyun SJ, Lenke LG, Kim YC, Koester LA, Blanke KM (2014) Comparison of standard 2-rod constructs to multiple-rod constructs for fixation across 3-column spinal osteotomies. Spine 39(22):1899–1904
13. Deviren V, Tang JA, Scheer JK, Buckley JM, Pekmezci M, McClellan RT, Ames CP (2012) Construct rigidity after fatigue loading in pedicle subtraction osteotomy with or without adjacent interbody structural cages. Glob Spine J 2(4):213–220
14. Smith JS, Shaffrey CI, Ames CP, Demakakos J, Fu K-MG, Keshavarzi S, Li CMY, Deviren V, Schwab FJ, Lafage V, Bess S (2012) Assessment of symptomatic rod fracture after posterior instrumented fusion for adult spinal deformity. Neurosurgery 71(4):862–867
15. Januszewski J, Beckman JM, Harris JE, Turner AW, Yen CP, Uribe JS (2017) Biomechanical study of rod stress after pedicle subtraction osteotomy versus anterior column reconstruction: a finite element study. SNI Spine 8:207
16. La Barbera L, Brayda-Bruno M, Liebsch C, Villa T, Luca A, Galbusera F, Wilke HJ (2018) Biomechanical advantages of supplemental accessory and satellite rods with and without interbody cages implantation for the stabilization of pedicle subtraction osteotomy. Eur Spine J 27(9):2357–2366
17. Hallager DW, Martin G, Dahl B, Harris J, Gudipally M, Jenkins S, Wu AM, Bucklen B (2016) Use of supplemental short precontoured accessory rods and cobalt chrome alloy posterior rods reduces primary rod strain and range of motion across the pedicle subtraction osteotomy level: an in vitro biomechanical study. Spine 41(7):E388–E395
18. Sellei RM, Kobbe P, Dadgar A, Pfeifer R, Behrens M, von Oldenburg G, Pape HC (2015) External fixation design evolution enhances biomechanical frame performance. Injury 46(Suppl 3):23–26
19. Finlay JB, Moroz TK, Rorabeck CH, Davey JR, Noume RB (1987) Stability of ten configurations of the Hoffmann external-fixation frame. J Bone Joint Surg Am 69(5):734–744
20. Cahill PJ, Wang W, Asghar J, Booker R, Betz RR, Ramsey C et al (2012) The use of a transition rod may prevent proximal junctional kyphosis in the thoracic spine after scoliosis surgery: a finite element analysis. Spine 37:E687–E695
21. Wilke HJ, Wenger K, Claes L (1998) Testing criteria for spinal implants: recommendations for the standardization of in vitro stability testing of spinal implants. Eur Spine J 7(2):148–154
22. Jager ZS, İnceoğlu S, Palmer D, Akpolat YT, Cheng WK (2016) Preventing instrumentation failure in three-column spinal osteotomy: biomechanical analysis of rod configuration. Spine Deform 4(1):3–9
23. Luca A, Ottardi C, Sasso M, Prosdocimo L, La Barbera L, Brayda-Bruno M, Galbusera F, Villa T (2017) Instrumentation failure following pedicle subtraction osteotomy: the role of rod material, diameter, and multi-rod constructs. Eur Spine J 26:764–770
24. Korupolu SC, Daniels AH (2018) Biomechanical comparison between titanium and cobalt chromium rods used in a pedicle subtraction osteotomy model. Orthop Rev 10(1):7541

25. Luca A, Ottardi C, Lovi A, Brayda-Bruno M, Villa T, Galbusera F (2017) Anterior support reduces the stresses on the posterior instrumentation after pedicle subtraction osteotomy: a finite-element study. Eur Spine J 26(Suppl 4):450–456
26. Berjano P, Blanco JF, Rendon D, Villafañe JH, Pescador D, Atienza CM (2015) Finite element analysis and cadaveric cinematic analysis of fixation options for anteriorly implanted trabecular metal interbody cages. Eur Spine J 24(7):918–923